Macroscopic simulation of the liner honing process

Benoit Goeldel [a,c,*], Mohamed El Mansori [a], Didier Dumur (1)[b]

[a] Arts & Métiers Paris Tech, LMPF, EA 4106, Châlons-en-Champagne, France
[b] SUPELEC Systems Sciences (E3S) EA 4454, Control Department, Gif-sur-Yvette, France
[c] Renault S.A.S. Powertrain Division, Rueil Malmaison, France

Keywords:
Honing
Grinding
Simulation

A B S T R A C T

The form quality, the roughness and the surface appearance produced by honing minimizes the friction of the piston in the liner. The process is however mechanically complex and the selection of the process parameters is currently based on empirical methods. The aim of this paper is thus to develop a macroscopic simulation environment of complete real honing cycles, which will help end-users during the setting-up. This virtual tool is based on a space–time discretization and a macroscopic cutting model taking into account local contacts between the workpiece and the abrasive tool. The space–time discretization allows representing the machine environment with the tool, the workpiece and the kinematics. Simulation results are finally validated by comparison with industrial experiments.

1. Introduction

Cylinder bore honing is a multi-stage metal removal process usually used after boring to obtain precise bore geometry and a specific surface finish. Material removal is ensured by pushing abrasive stones against the workpiece [1].

The honing stones movement generates a helical pattern with a characteristic crosshatch angle determined by the relative spindle and stroke speeds [2].

The honed surface in engine cylinder liner plays an important role on its functional features and contains qualitative characteristics [3,4]. The generation of these surfaces is monitored by a great number of process parameters defined by empirical setting up methods.

Many attempts have been made by researchers to develop numerical simulation methods for manufacturing processes, e.g. [5,6]. This task is also not so easy because honing involves graduated stages of abrasive finishing processes, using at first coarse abrasive stones, and then progressively finer grades [7,8].

Actually, industrialists have to test different setting configurations to find the best one for the requested quality. To minimize this tuning phase, this paper proposes the elaboration of a honing model linking the machine parameters to the process results and the industrial quality index. Each stage of the process will be thus successively simulated. The final aim of this simulation is to assist end-users in the choice of the appropriate machine parameters to obtain the specified quality in terms of form, roughness and surface aspect.

It is based on a new method to simulate the specific process of cylinder engine honing. This macroscopic approach is useful to increase the process understanding and improve the abrasive process knowledge.

* Corresponding author.

2. Kinematics and force simulation

The derived method is based on the philosophy developed in [10]. The proposed simulation model will be elaborated coupling an abrasive cutting model and a spatiotemporal discretization that allows integrating the tool kinematics relatively to the workpiece.

2.1. Kinematics simulation: spatiotemporal discretization

The first action is to choose a mesh which allows introducing a macroscopic view of the cylinder and a micro definition of the surface quality. For that, classical 3D mesh cannot be used. The third dimension, the radial thickness, is too small compared to the cylinder height and diameter. Therefore, it has been chosen to collect each value of the material thickness and the roughness in matrix of appropriate dimension: each cell of the matrix represents a small square (dX^*dX) of the internal cylinder surface.

Globally, several matrices are defined. Data in the two first matrices of the cylinder represent the thickness of remaining material with or without the local maximum roughness. Data corresponding to the orientation of the cutting speed are collected in other matrices so-called "orientation matrices".

Specific roughness and form default scanned on a real carter with the metrology machine are introduced as initialization values.

The time-domain discretization will be directly dependent on the mapping definition and the main direction of cut. Denoting dX (m) the size definition of the mesh tile, D (m) the mean diameter of the cylinder bore, Va (m/s) the stroke speed and N (rpm) the angular velocity of the tool, the sampling period related to this discretization is defined by τ (s):

$$\tau = \min\left(\frac{60 \times dX}{\pi \times D \times N}; \frac{dX}{Va}\right) \quad (1)$$

Trajectories are defined as for the real machine: all parameters of the stroke movement (inversion point positions, speed, acceleration) and the rotation speed can be easily set.

At each time instant, the two matrices are overlaid with the new position corresponding to the selected honing parameter kinematic. For each mesh tile where there is contact between the stone and the workpiece, the proposed abrasive action model is applied. From this information, the local number of stone passage is integrated and the map of stone number passage distribution is created.

2.2. Force simulation: abrasive contact pressure calculation

The honing machine has two stone expansion systems, which allow connecting the stones and the workpiece: an electromechanical expansion, which consists in using the stone position control, and a hydraulic expansion, which uses upward thrust control. Both of them are integrated in the simulator, with the hypothesis that stones cannot rotate on their stands and the tool is naturally well centered in the cylinder.

For electromechanical expansion simulation, only the new radial dimension of the tool is calculated for each abrasive mesh tile and the local stone pressure is derived. This local value is defined by the workpiece characteristics, the stone thickness and the value of the stone radial expansion. In the case of hydraulic expansion system, the local stone pressure is calculated with a special pressure repartition algorithm. Knowing the stone elements in contact, the global pressure is therefore distributed as a function of stone and workpiece thicknesses.

By integrating the local contact pressure for every stone mesh tile, the global radial force is obtained. In the case of hydraulic expansion, this force is naturally the same as specified by the machine. In the case of electromechanical expansion, the simulation gives us the force developed by the electric actuator.

Assuming that the friction between tool and cylinder is dry, and denoting f_1 the axial friction coefficient, the axial forces are calculated as follows:

$$F_r(t) = (dX)^2 \cdot \sum_{i,j} P_c(i,j)(t) \tag{2}$$

$$F_a(t) = sign\,(Vb(t)) \cdot f_1 \cdot F_r(t) \tag{3}$$

To identify this coefficient that must be integrated in the simulator, the only available measurement is the axial force. Therefore, based on experimental axial force results and using simulated radial force, the calculated axial friction coefficients f_1 ($=F_a/F_r$) is given in Table 1.

3. Cutting model

A macroscopic model of abrasive cutting is developed below. For a specific couple of abrasive stone and workpiece material, the factors which influence the removal material and the honed surface quality are cutting speed and stone pressure [1]. Therefore, measuring the stock removal and the stone wear at different couples of speed and pressure enables to deduce this predictive model.

Following the work of Sasaki and Okamura [9], the predictive model is generated with a function as simple as possible. In the literature, experiments proved that stock removal is a linear function of contact pressure for the same cutting speed, in the middle of the range. For a fixed stone pressure, the stock removal depends only of cutting speed. In the middle of the cutting speed range, stock removal is a linear function of contact pressure.

The stock removal SR appears thus to be a bi-linear function of stone pressure P and cutting speed Vc within a certain range close to the optimum. This fact is expressed by the following equation, where u, v, and w are constants depending on stone and workpiece materials.

$$SR = u \times P + v \times Vc + w \times P \times Vc \tag{4}$$

Table 1
Axial friction coefficient identification.

Abrasive type	Peak radial force [N]	Peak axial force [N]	Friction coefficient
SiC-IAS65/120/1/8Vs	480	390	0.813
SiC-SCG600KE 20 6469	320	280	0.875

Table 2
Results of removal rate experiences.

Abrasive type	Cutting speed (Vc) [m/min]	Expansion pressure [10^5 Pa]	Removal material [mm^3]	Cycle time [s]	Removal rate [$mm^3/s/mm^2$]
SiC-IAS65/120/1/8Vs	40	~18[a]	688.28	22.10	0.019
	40	~30[a]	809.53	17.85	0.027
	40	~36[a]	595.98	11.19	0.032
	50	~21[a]	693.07	14.67	0.028
	50	~27[a]	784.05	14.73	0.032
	50	~35[a]	652.81	10.46	0.037
	60	~22[a]	655.61	18.61	0.021
	60	~28[a]	658.13	10.30	0.038
	60	~37[a]	402.67	5.24	0.046
SiC-SCG600KE 20 6469	40	3	1068.8	52.06	0.012
	40	3.75	1150.4	54.26	0.01262
	40	5.25	1625.5	71.60	0.01351
	50	4.5	1699.7	80.92	0.01250
	50	6	1469.6	69.87	0.01252
	50	7.5	1989.9	93.69	0.01264
	60	4.5	1388.0	67.41	0.01226
	60	6	1707.1	81.28	0.01250
	60	7.5	2293.2	107.5	0.01269

[a] Average equivalent expansion pressure value measured with monitoring system.

3.1. Identification of coefficients of the stock removal equation

For the established abrasive regime, a series of experiments has been conducted to determine the stock removal rate as a function of expansion pressure and cutting speed for each type of abrasive used in our honing process. The same method as in [1] was used to determine the stock removal: the diameters before and after a simple stage honing are measured, the volume of the stock removal is also calculated. Knowing the tool geometry with the abrasive and the time cycle, the stock removal rate is then calculated for the honing process condition.

Table 2 gives the different results obtained to calculate the primary input to the cutting model of the honing simulation.

Based on this, it has been checked that the previous experimental stock removal results can be extrapolated to a large range of stock removal. Table 3 presents the coefficients u, v, w identified from these results by linear regression for each type of abrasive stone.

3.2. Roughness model

Only the local maximum roughness (Rz) is represented and modified at each iteration, in case of removed material. Seven cases of roughness modification have to be distinguished, depending on the local penetration deepness. The abrasive indentation (Tg) is a third of the grit size. As an example, in Fig. 1, in case A1, the penetration deepness (U) is lower than (Tg) and lower than the local roughness (Rz).

Table 3
Abrasive cutting coefficients identified from experiences.

	u	v	w
SiC – IAS65/120/1/8Vs	3.72E−04	2.69E−05	−5.05E−06
SiC – SCG600KE 20 6469	9.08E−04	1.40E−04	−3.54E−06

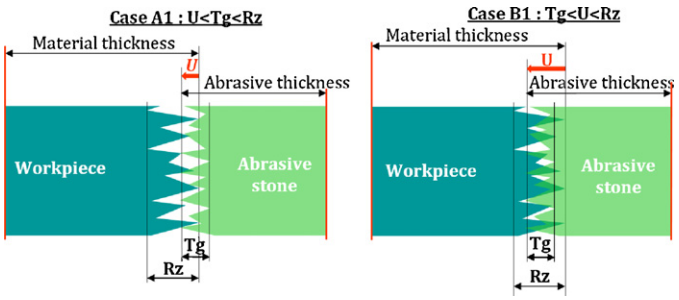

Fig. 1. Two different cases of penetration mode.

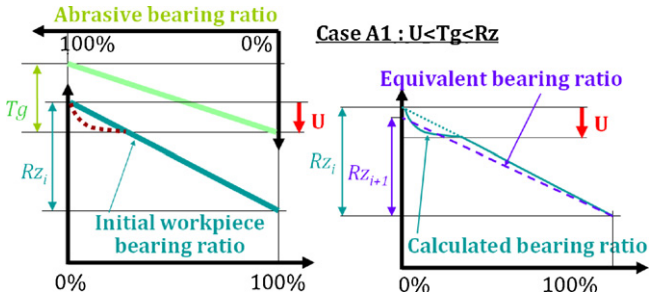

Fig. 2. Bearing ratio and roughness calculation.

The bearing area ratio of the workpiece ($T\%_F$) and the bearing area ratio of the abrasive stone ($T\%_R$) are assumed to be linear. In the case A1, illustrated in Fig. 2, for the radial abscissa x, these ratios are given by (5). In the interaction zone, the new bearing ratio of the workpiece is deduced by (6).

$$T\%_R = \frac{Tg - x}{Tg} \text{ and } T\%_F = \frac{x - Tg + U}{Rz} \tag{5}$$

$$T\%_F^{\text{interact}}(x) = T\%_F(x) \times (1 - T\%_R(x)) \tag{6}$$

But it is not a linear function of x. To find the linear bearing ratio equivalent to the interaction bearing ratio, the remaining material volume is equalized as in (7) and the new roughness resulting for case A1 is Rz_{i+1} given by (8).

$$\oint T\%_F^{\text{equi}} \cdot dx = \int_{Tg-U}^{Tg} T\%_F^{\text{interact}}(x) \cdot dx + \int_{Tg}^{Tg-U+Rz_i} T\%_F(x) \cdot dx = \frac{Rz_{i+1}}{2} \tag{7}$$

$$Rz_{i+1} = Rz_i - \frac{U^3}{3 \cdot Tg \cdot Rz_i} \tag{8}$$

The same method is used to calculate the new equivalent roughness for the six other cases of penetration.

4. Simulation results and experimental comparison

This section now focuses on the results of the simulation and compare them to experimental records.

4.1. Simulated and measured axial forces

Fig. 3 illustrates during one stroke period the signal coming from the strength sensor and the simulated axial force. They appear to have the same profile and as expected the friction coefficient f_1 acts as a gain for the simulated force.

This experiment shows that the signal form and the pattern are only influenced by the process geometry and kinematics, meaning that the hypothesis of dry friction for axial movement is valid.

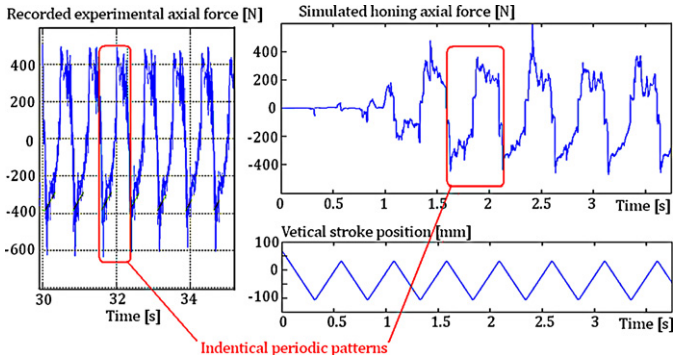

Fig. 3. Axial forces comparison for silicium carbide abrasive.

4.2. Cycle time forecast

The cycle time is uncertain because cylinders are all different. Cylinder diameters are within a large tolerance interval. This may induce more material removed to get the final diameter. The honing tool is equipped with blowing nozzles for in-process measuring. It enables to simulate the "macro-form corrector" of the real machine. The honing machine records three diameters at three different levels defined by the user. If one of the diameter scan is too small compared to the other ones, the machine makes some short stroke movements on small diameter zone until the diameter is as large as the others. Short strokes could lengthen the cycle time, so it is important to take into account this functionality to forecast it. Numbers of short strokes in Table 4 show that the simulated behavior is similar to the one with the real corrector. The use of the macro-form corrector and the diversity of different input cylinder form create an additional hazard on cycle time. To be closer to the reality special thickness matrices are created integrating real form default. The study of the evolution of the global cylinder form is then carried out by simulating honing on real scan cylinder.

The experiment consists in making the rough honing on 36 cylinder bores. The quality form and diameters were measured before. The cylinders of type A have a deformity similar to a barrel and of type B similar to a cone. Scanned points issued from the measurement machine are used to create the matrix mesh of the cylinder.

In Table 4, the cycle time and number of activation of the macro form corrector are compared during the cycle.

The slight difference between real and simulated cycle time illustrates the validity of the developed cutting model.

4.3. Roughness forecast

The finishing is a honing process stage designed to reduce the roughness and to generate a surface texture with cross grooves.

This stage essentially simulates the roughness evolution and the cylinder form quality. The most interesting finish honing result is the roughness map. This map is of great interest, showing an approximate roughness for each point of the cylinder surface. However, the simulation results will be compared below with the experiments only in three points, because the roughness measurements are heavy to implement.

Table 4
Cycle time comparison for rough honing with and without macro form corrector.

Cycle time comparison with expansion speed at 6 μm/s						
Initial form default	Cutting speed [m/min]	Macro-form corrector	Cycle time		Number of short strokes	
			Meas.	Sim.	Meas.	Sim.
Type A (><)	55	No	32.4s	33s	0	0
	55	Activate	37.8s	38s	3	4
Type B (/\)	55	No	29.8s	30s	0	0
	55	Activate	39.2s	40s	5	5

Meas.: experimental measurements; Sim.: simulation results.

Table 5
Roughness criterion comparison between simulation and experiments.

Experiment	Cutting speed [m/min]	Expansion speed [μm/s]	Groove cross angle [°]	Accel. of stroke inversion [m/s^2]
Type I	40	3.5	50	15
Type II	40	3.5	50	10
Type III	40	3.5	50	5

Experiment	Roughness Rz level 1 [μm]		Roughness Rz level 2 [μm]		Roughness Rz level 3 [μm]	
	Meas.	Sim.	Meas.	Sim.	Meas.	Sim.
Type I	6.52 ± 0.35	6.5	6.06 ± 0.47	6.0	6.47 ± 0.35	6.6
Type II	7.20 ± 0.46	7.0	6.58 ± 0.36	6.3	7.30 ± 0.36	7.1
Type III	7.57 ± 0.36	7.7	7.38 ± 0.34	6.8	9.06 ± 0.37	8.0

Table 6
Form default comparison between simulation and experiments.

Experiment	Cylindricity [μm]		Straightness [μm]		Average roundness [μm]	
	Meas.	Sim.	Meas.	Sim.	Meas.	Sim.
Type I	10.91 ± 0.2	11.0	5.81 ± 0.2	5.9	5.90 ± 0.2	6.8
Type II	10.61 ± 0.1	10.5	5.75 ± 0.2	5.6	5.77 ± 0.2	6.0
Type III	10.57 ± 0.3	10.0	5.61 ± 0.2	5.3	5.60 ± 0.2	5.3

Meas.: experimental measurements; Sim.: simulation results

Therefore, Table 5 compares the Rz roughness measured experimentally at three different heights of the cylinder and the value of the roughness map for those points.

The cylinder form simulated is generated from the real cylinder form scanned after the rough honing stage. The form evolution is also compared during this stage. The experiment involves 18 samples grouped into three categories. Comparison between experiment and simulation form quality results is presented in Table 6.

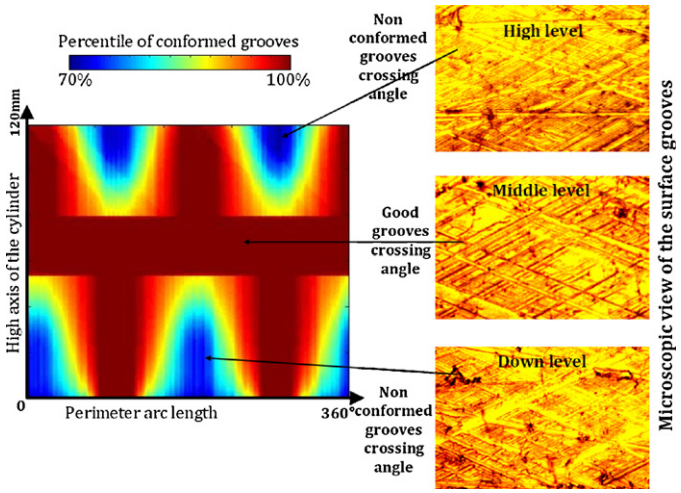

Fig. 4. Simulated surface aspect mapping versus real views of honed cylinder.

4.4. Macro texture quality forecast

Another criterion of interest is the surface appearance formed by crossing grooves. The surface appearance is forecasted by calculating and recording the direction of stone passages for each mesh tile and during all the finish honing and plateau honing time. Only directions associated to a positive local stock removal and with a near end remaining stock thickness are taken into account during the compilation of the surface aspect map.

Criteria of surface aspect quality are currently defined by human view analysis and there is no numerical index. The importance of the grooves cross angle is known from the experiences. These criteria are thus considered to evaluate the simulation. Fig. 4 shows views from well crossed and non conformed zones determined by the simulation and the real microscopic views, in complete agreement.

This stage simulation could easily forecast recommended cycle time to obtain a homogenous appearance all over the cylinder surface. This simulation is the only one to predict such criteria.

5. Conclusion

This paper introduces a functional approach of the honing process simulation. The macroscopic model is useful for generation of honed surface maps. The kinematics module can easily calculate the stone passage number map and determine local contacts between abrasive and workpiece at each instant of the honing cycle. The force module coupled with the cutting model allows determining the stock removal and the map of the stock remaining thickness. The choice of the tool geometry and the honing kinematics could be therefore optimized in order to have the best uniform honing surface.

The definition of stock removal in the cylinder bore allows determining the strokes number and the cycle time needed to achieve the requested form quality and roughness. Combining number of stone passage, cutting orientation and thickness of the latest stone passage, enables to create the surface aspect mapping. This mapping helps manufacturers to set up optimized stroke parameters, such as acceleration and stroke amplitudes.

To conclude, this macroscopic simulation can forecast macro and micro geometry criteria by taking into account cylinder and tool geometry and the initial roughness and the grit size. Results obtained with this simulation encouraged us to continue with this type of mesh. But the use of a 3D mesh of the whole carter allows calculating the geometrical deformation. By coupling the 2D honing simulation with a 3D FEM of the engine bloc, the simulation will be able to calculate the instantaneous deformation during the honing process.

References

[1] Sabri L, El Mansori M (2009) Process Variability in Honing of Cylinder Liner with Vitrified Bonded Diamond Tools. *Surface & Coatings Technology* 204:1046–1050.

[2] Voronov SA, Gouskov AM, Bobrenkov OA (2009) Modelling of Bore Honing. *International Journal of Mechatronics and Manufacturing Systems* 2(5/6): 566–575.

[3] Haasis G, Weigmann U-P (1999) New Honing Technique Reduces Oil Consumption. *Industrial Diamond Review* 3(99):205–211.

[4] Santochi M, Vignale M, Giusti F (1982) A Study of the Functional Properties of Honed Surface. *Annals of the CIRP* 31(1):431–434.

[5] Torrance AA (2005) Modelling Abrasive Wear. *WEAR* 258:281–293.

[6] Tönshoff HK, Peters J, Inasaki I, Paul T (1992) Modelling and Simulation of Grinding Processes. *Annals of the CIRP* 41(2):677–687.

[7] Sabri L, Mezghani S, El Mansori M, Zahouanic H (2010) Multiscale Study of Finish-honing Process in Mass Production of Cylinder Liner. *WEAR* 271:509–513.

[8] Lee J, Malkin S (1993) Experimental Investigation of the Bore Honing Process. *Transactions of the ASME* 115:406–414.

[9] Sasaki T, Okamura K (1959) The Cutting Mechanism of Honing. *Japan Society of Mechanical Engineers* 2(5):80–85.

[10] Chen X, Rowe WB (1996) Analysis and Simulation of the Grinding Process. Part II. Mechanics of Grinding. *International Journal of Machine Tools Manufacturing* 36(8):883–896.